Distribution Functions of Positive Ions and Electrons in a Plasma Near a Surface

Peng-Sheng Wei, *Member, IEEE*, Feng-Bin Yeh, and Ching-Yen Ho

***Abstract*—In this study, the velocity distribution functions of the ions and electrons in a collisional presheath and collisionless sheath of a plasma near a wall emitting and reflecting ions and electrons are systematically determined. The collisions in the presheath are modeled by a relaxation time approximation (namely, Bhatnagar–Gross–Krook model, or simply BGK model). To find the variation in electrostatic potential with position, the model and analysis from Emmert *et al.*are used. Distribution functions of the ions and electrons in a collisionless presheath and sheath on a wall partially reflecting ions and electrons, therefore, can be exactly obtained. The reflections of the ions and electrons by a wall play important roles in studying heat transfer from a plasma sheath to a workpiece surface, and sputter etching and deposition, ion implantation, and ion scattering spectroscopy. Irrespective of ion and electron reflectivities, velocities of the ions in the presheath and sheath are of highly non-Maxwell–Boltzmann distributions. The electrons in the presheath are close to Maxwell–Boltzmann distributions, whereas those in the sheath are non-Maxwell–Boltzmann distributions. Even though the wall partially reflects ions and electrons, the Bohm's criterion is marginally satisfied at the sheath edge. The computed distribution functions for a completely absorbing surface agree with theoretical results provided in the literature. Good comparison of the resulted transport variables with available analytical work is presented in the companion paper.**

***Index Terms*—Kinetic analysis of plasma, plasma materials processing, plasma-wall interactions, space charge.**

NOMENCLATURE

c	Particle thermal speed, $c^* = c/(k_B T_{e0}/m_i)^{1/2}$.
c_0	$(-2Z_i e\phi/m_i)^{1/2}$.
c_0'	$[2Z_i e(\phi_b - \phi)/m_i]^{1/2}$.
D	Dawson function, as defined in (40).
e	Electron charge.
f, F, g	Ion distribution function, $F^* = F(k_B T_{e0}/m_i)^{1/2}/n_{e0}$.
H	Heaviside function, $H(x) = 1$ for $x > 0$; $H(x) = 0$ for $x < 0$.
I, K	Function defined in (37) and (32).
k_B	Boltzmann constant.
m	Particle mass.
n	Particle density, $n^* = n/n_{e0}$.
S	Ion source, defined in (30).
T	Temperature.
x, y, z	Cartesian coordinate.
Z	Charge number.

Greek Letters

β	Collision parameter.
ε	Total energy.
κ	T_{e0}/T_{i0}.
ρ	Reflectivity.
σ	$c_x/\lvert c_x\rvert$.
ϕ, χ	Dimensional and dimensionless potential, $\chi = -e\phi/k_B T_{e0}$.
χ_t	$-\varepsilon/(Z_i k_B T_{e0}) = -m_i c_x^2/(2Z_i k_B T_{e0}) + \chi$.
ε_t	$Z_i e\phi$.
λ	Mean free path.

Superscript

$*$	Dimensionless quantity.

Subscript

b	Boundary between sheath and presheath.
e, i	Electron and ion.
t	Turning point.
w	Wall.
$0, 1$	Coordinate origin at $\phi = 0$ and sheath edge, as illustrated in Fig. 1.

Manuscript received April 16, 1999; revised March 14, 2000. This work was supported by the National Science Council, R.O.C., under Grant NSC 87-2212-E-110-029.

P.-S. Wei and F.-B. Yeh are with the Department of Mechanical Engineering, National Sun Yat-Sen University, Kaohsiung, Taiwan 80424, R.O.C. (e-mail: pswei@mail.nsysu.edu.tw).

C.-Y. Ho is with the Hwa Hsia College of Technology and Commerce, Taipei, Taiwan, R.O.C.

Publisher Item Identifier S 0093-3813(00)07248-9.

I. INTRODUCTION

THE plasma induced in metals processing is usually accompanied by strong momentum and energy transport near the workpiece surface. Owing to different thermal speeds of the ions and electrons, a sheath or space-charge region in a thin layer exists on the surface [1]. The function of the sheath is to form a potential barrier so that the flux of electrons that have enough energy to go over the barrier to the wall is just equal to the flux of ions reaching the wall. Regardless of the Debye shielding, small electrostatic potential in the presheath between the sheath and bulk plasma still accelerates the ions up to and beyond sonic speed before entering the sheath, as first explicitly pointed out by Bohm [2].

An accurate study of transport processes for a plasma near a wall requires a kinetic analysis, that is, to solve velocity distribution functions of the ions and electrons from Boltzmann's equations coupled with Poisson's equation. One of the earliest kinetic analyzes of a bounded, quasineutral, collisionless plasma for a gaseous discharge was performed by Tonks and Langmuir [3]. An integrodifferential plasma equation for a planar, cylindrical, and spherical plasma consisting of warm electrons

($T_e \neq 0$) and cool and cold ions ($T_i/T_e \ll 1$ and $T_i = 0$) by choosing different ion source functions was derived. The solutions were found in series of infinitesimal Debye length for various ratios of ion mean-free path to characteristic length of the plasma [4]. The collision-free low-pressure column was experimentally confirmed by the free fall of the ions originating from ionization of the cold neutrals.

Harrison and Thompson [5] solved exactly the plasma equation obtained from Tonks and Langmuir [3] by introducing an ion source function indicating that all ions were generated with zero speed. Interestingly, the resulted potential and current density at the sheath edge were found to be independent of spatial variations in ion sources. Rather than the monoenergetic distribution at ion temperature $T_i = 0$ as used by Bohm [2], they found a generalized Bohm's criterion, which was valid for any velocity distribution of ions at the sheath edge.

The first model to study warm ions in a presheath was proposed by Hu and Ziering [6], who assumed that velocities of the ions at the plasma–sheath interface were of accelerated, cutoff, and drifted Maxwell–Boltzmann distributions. The results lead to another generalized Bohm sheath criterion, which reduced to the Bohm's original inequality in the limit $T_{i0}/T_{e0} \rightarrow 0$. Emmert *et al.* [7] extended the analysis of Hu and Ziering [6] to obtain a more realistic noncutoff ion distribution function in a collisionless presheath near a completely absorbing and floating wall. The ion source function was chosen such that the ions would be of a Maxwell–Boltzmann distribution in the absence of electrostatic field. Because no ions were produced with zero speed in this model, this study first successfully confirmed that the ions were satisfied by a finite electrostatic field and generalized Bohm criterion at the sheath edge [8], [9]. Physically speaking, the ions must be accelerated from their initial speeds by the electric field. Provided that the ions were generated with zero speed under charge neutrality, the electric field at the sheath edge would become infinitely large to force the ions to reach a sonic speed [8]. Surprisingly, in the limit of infinitesimal ratio of the Debye length to macroscopic length of the system, the resulting "warm" plasma equation by a transformation became the "cold" plasma equation treated by Harrison and Thompson [5]. Potential ion and total energy fluxes at the sheath edge, therefore, were analytically and exactly found. Aside from the potential curve cutoff at a new sheath edge, the predicted mass and total energy fluxes were different from those obtained from a half-space Maxwell–Boltzmann distribution.

Bachet *et al.* [10] measured the ion distribution functions of an argon plasma at pressures of 0.08 and 0.013 Pa and densities between 10^{14} and 10^{15} particles/m^3 with a laser-induced fluorescence. The experimental findings showed good agreement with the solutions of Emmert *et al.* [7] by adjusting ion temperatures between 2000 and 43 000 K in a trend decreasing with distance from the wall. It was observed that the ion distribution function at any location in the presheath can be divided by three parts agreeing with the prediction made by Emmert *et al.* [7]. The first part was referred to the ions coming from the presheath edge and the ions created in the presheath. The middle part was for the low-energy ions generated with positive velocities in the backward region and negative velocities in the entire presheath. The left part was composed of high-energy ions originated with negative velocities in the forward region. Although the ion distribution functions were consistent, temperatures of ions should be around the ambient temperature as presented by Goeckner *et al.* [11]. One possible reason for this discrepancy is a neglect of ion-neutral collisions.

In this study, general velocity distribution functions of the ions and electrons in a collisional presheath and collisionless sheath of a plasma near a wall emitting and reflecting ions and electrons are derived. Extending the model and analysis from Emmert *et al.* [7] to find the variation in electrostatic potential with position, distribution functions of the ions and electrons in a collisionless presheath and sheath on a wall partially reflecting ions and electrons can be obtained. The reflections of the ions and electrons play important roles in studying heat transfer from a plasma sheath to a workpiece [12] and sputter etching and deposition, ion implantation, and a technique known as ion scattering spectroscopy [13]. Transport variables of ions and electrons in the plasma near the wall can be accurately obtained from the moments of the distribution functions in the companion paper [14].

II. Kinetic Model and Analysis

The plasma comprising the bulk plasma, presheath, and sheath near walls is illustrated in Fig. 1. The origin of the coordinate is conveniently set at the edge of the presheath or bulk plasma, where electrostatic potential is zero. The quasineutral presheath is an ionization zone to supply ions lost to walls. Because electrostatic potential decreases, the ions in the positive x-direction are accelerated, whereas backward-moving ions are decelerated. The decelerated ions with total energy less than zero experience turning. On the other hand, the electrons in the positive direction need to overcome potential. An electron with the total energy less than wall potential turns to the presheath before hitting the wall. In this study, the major assumptions made are as follows.

1) Transport processes in the presheath and sheath can be considered in a quasisteady state [1], [7], [13]. In reality, this is only the average result of the many detailed interactions among particle–particle, wave–particle, and wave–wave, such as plasma oscillations, oscillations of kinetic, two-stream and parametric decay instabilities, and the effects of Landau damping, and so on [1]. The electrostatic potential can also have spatial and temporary oscillations and trap particles. In practice, dissipative processes tend to destroy oscillations.
2) The ion collisions are simulated a relaxation time approximation as first proposed by the Bhatnagar–Gross–Krook (BGK) model [15] to replace the complicated collision integral. The BGK model treating a binary collision simplifies the mathematical manipulation but retains many of the features of the true collision integral. The collision model needs to satisfy conservation of particle, momentum, and energy. When a charged particle undergoes a large number of small deflections in the force field of many charged particles, a more realistic and complicated Fokker–Planck collision term can be used.

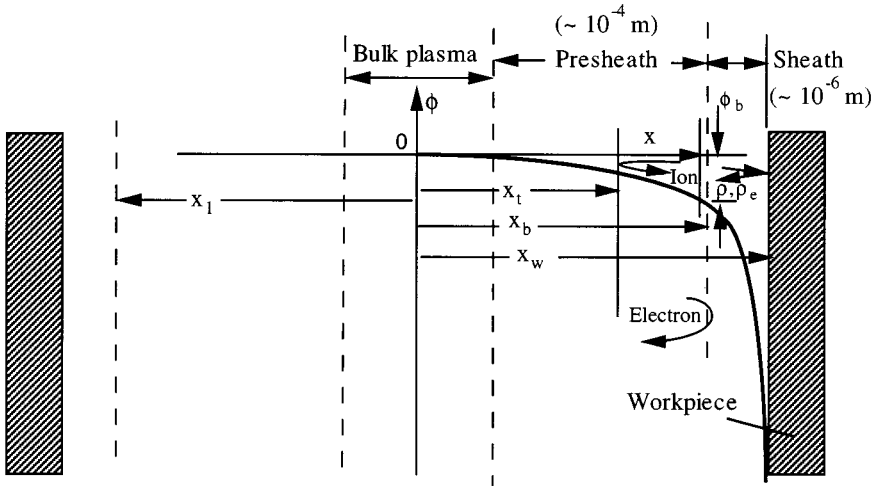

Fig. 1. System model and coordinates.

3) Electromagnetic force (namely, Lorentz force) is ignored. This is valid for the cases in which magnetic field is negligible or the direction of magnetic lines is parallel to the ion flow. Neglect of the magnetic field is due to a greater Larmor radius than the thickness of the presheath. Larmor radius is a measure of the radius of the helical path of a charged particle. For a typical magnetic flux density less than 0.1 tesla [16], Larmor radius is greater than 5×10^{-3} m.
4) Reflectivities of electrons and ions are constant and independent of energy.

A. Ion Distribution Functions

With the above assumptions, the Boltzmann equation integrated over velocity component c_y and c_z yields

$$c_x\frac{\partial F_i}{\partial x}-\frac{Z_ie}{m_i}\frac{d\phi}{dx}\frac{\partial F_i}{\partial c_x}=S_i(x,c_x)+\nu(F_{i0}-F_i) \quad (1)$$

where the ion distribution function and source terms are

$$F_i(x,c_x)=\int_{-\infty}^{\infty} f_i\,dc_y\,dc_z$$
$$S_i(x,c_x)=\int_{-\infty}^{\infty} S_i\,dc_y\,dc_z. \quad (2)$$

The last term on the right-hand side of (1) represents collisions simulated by the BGK model [15], [17], where ν is collision frequency, and distribution function F_{i0} is the Maxwell-Boltzmann distribution function. Equation (1) can be conveniently expressed by independent variables of position x and total energy ε

$$\frac{\partial}{\partial x}\left[\sigma|c_x|g(x,\varepsilon,\sigma)\right]=S_i(x,\varepsilon,\sigma)+\frac{\nu}{\sigma m_ic_x}(F_{i0}-F_i) \quad (3)$$

where the total energy is

$$\varepsilon=\tfrac{1}{2}m_ic_x^2+Z_ie\phi(x) \quad (4)$$

Because energy is a scalar, the quantity $\sigma\equiv c_x/|c_x|$ is introduced to account for the direction of velocity. The velocity distribution function and source function of ions in (3) are, respectively, defined as

$$g(x,\varepsilon,\sigma)\equiv\frac{\sigma F_i(x,c_x)}{m_ic_x}$$
$$S_i(x,\varepsilon,\sigma)=S_i(x,c_x)\frac{dc_x}{d\varepsilon}=\frac{S_i(x,c_x)}{\sigma m_ic_x}. \quad (5)$$

B. Presheath

To determine ion distribution functions in the presheath, (3) can be written as

$$\frac{\partial}{\partial x}\left[\sigma|c_x|g(x,\varepsilon,\sigma)\right]=A(x,\varepsilon,\sigma)-\nu g(x,\varepsilon,\sigma) \quad (6)$$

where the ion source function $A\equiv S_i+\nu F_{i0}/(m_i|c_x|)$ is symmetric with respect to zero velocity, namely, $A(x,\varepsilon,+1)=A(x,\varepsilon,-1)$ [17]. Boundary conditions of (6) are $g(x_1,\varepsilon,+1)=g_1(\varepsilon,+1)$, and $g(x_b,\varepsilon,-1)=g_b(\varepsilon,-1)$. Equation (6) can be readily integrated to obtain the ion distribution function. Because the ion distribution function also depends on if positive ions moving in the negative direction experience turning, two different cases are considered as follows.

1) Ion distribution functions for total energy $\varepsilon>0$. The distribution function of the ions moving in the forward direction yields

$$|c_x|g(x,\varepsilon,+1)=g_1(\varepsilon,+1)\,|c_{x_1}|\,e^{-(\beta x-\beta_1x_1)}+\int_{x_1}^{x}A(x',\varepsilon,+1)e^{-(\beta x-\beta' x')}\,dx' \quad (7)$$

where variable β represents the mean value of collisions or the reciprocal of ion mean-free path within a distance x. Equation (7) indicates that the ion distribution at location x is determined by the ions of a distribution function g_1 at the boundary x_1 and the ions generated between x_1 and x. The distribution function for negative velocities is

$$|c_x|g(x,\varepsilon,-1)=g_b(\varepsilon,-1)\,|c_{x_b}|\,e^{-(\beta_bx_b-\beta x)}+\int_{x}^{x_b}A(x',\varepsilon,-1)e^{-(\beta' x'-\beta x)}\,dx' \quad (8)$$

which is determined by the ions of a distribution function $g_b(\varepsilon,-1)$ at the sheath edge and the ion generated between x and x_b, respectively.

2) Ion distributions functions for total energy $\varepsilon < 0$. The positive ions moving in the negative direction experiences turning. Ion distribution function for negative velocities is the same as (8), wheras that in the forward direction is

$$\begin{aligned}|c_x|g(x,\varepsilon,+1) &= g[x_t(\varepsilon),\varepsilon,+1]\,|c_{x_t}|\,e^{-(\beta x-\beta_t x_t)} \\ &\quad + \int_{x_t(\varepsilon)}^{x} A(x',\varepsilon,+1)e^{-(\beta x-\beta' x')}\,dx'. \end{aligned} \tag{9}$$

Conservation of the positive ion at the turning point is

$$|c_{x_t}|\,g[x_t(\varepsilon),\varepsilon,-1] = |c_{x_t}|\,g[x_t(\varepsilon),\varepsilon,+1]. \tag{10}$$

Equation (9), by introducing (10) and (8) evaluated at the turning point, leads to

$$\begin{aligned}|c_x|g(x,\varepsilon,+1) &= g_b(\varepsilon,-1)\,|c_{x_b}|\,e^{-(\beta_b x_b+\beta x-2\beta_t x_t)} \\ &\quad + \int_{x_t(\varepsilon)}^{x_b} A(x',\varepsilon,-1)e^{-(\beta' x'+\beta x-2\beta_t x_t)}\,dx' \\ &\quad + \int_{x_t(\varepsilon)}^{x} A(x',\varepsilon,+1)e^{-(\beta x-\beta' x')}\,dx' \end{aligned} \tag{11}$$

where the first two terms on the right-hand side refer to the ions moving in the negative direction and experiencing a turn at x_t. This can be clearly seen from the first term, in which dimensionless distance for collisions between x_b and x is $\beta_b x_b+\beta x-2\beta_t x_t = (\beta_b x_b-\beta_t x_t)+(\beta x-\beta_t x_t)$. The last term on the right-hand side of (11) is for the ions created in the upstream locations and directed in the positive direction. Regardless of total energy, distribution functions of the ions moving in the forward direction governed by (7) and (11) can be combined into one equation

$$\begin{aligned}|c_x|g(x,\varepsilon,+1) &= H(\varepsilon)\Big[g_1(\varepsilon,+1)\,|c_{x_1}|\,e^{-(\beta x-\beta_1 x_1)} \\ &\qquad + \int_{x_1}^{x} A(x',\varepsilon,+1)e^{-(\beta x-\beta' x')}\,dx'\Big] \\ &\quad + H(-\varepsilon)\Big[g_b(\varepsilon,-1)\,|c_{x_b}|\,e^{-(\beta_b x_b+\beta x-2\beta_t x_t)} \\ &\quad + \int_{x_t(\varepsilon)}^{x_b} A(x',\varepsilon,-1)e^{-(\beta' x'+\beta x-2\beta_t x_t)}\,dx' \\ &\quad + \int_{x_t(\varepsilon)}^{x} A(x',\varepsilon,+1)e^{-(\beta x-\beta' x')}\,dx'\Big]. \end{aligned} \tag{12}$$

The distribution function of the ions moving in the negative direction is (8). Combining ion distribution functions in both directions yields

$$\begin{aligned}\frac{F_i(x,c_x)}{m_i} &= H(c_x-c_0)\Big[g_1(\varepsilon,+1)\,|c_{x_1}|\,e^{-(\beta x-\beta_1 x_1)} \\ &\quad + \int_{x_1}^{x} A(x',\varepsilon,+1)e^{-(\beta x-\beta' x')}\,dx'\Big] \\ &\quad + H(c_x)H(c_0-c_x) \\ &\quad \times \Big[g_b(\varepsilon,-1)\,|c_{x_b}|\,e^{-(\beta_b x_b+\beta x-2\beta_t x_t)} \\ &\quad + \int_{x_t(\varepsilon)}^{x_b} A(x',\varepsilon,-1)e^{-(\beta' x'+\beta x-2\beta_t x_t)}\,dx' \\ &\quad + \int_{x_t(\varepsilon)}^{x} A(x',\varepsilon,+1)e^{-(\beta x-\beta' x')}\,dx'\Big] \\ &\quad + H(-c_x)\Big[g_b(\varepsilon,-1)\,|c_{x_b}|\,e^{-(\beta_b x_b-\beta x)} \\ &\quad + \int_{x}^{x_b} A(x',\varepsilon,-1)e^{-(\beta' x'-\beta x)}\,dx'\Big] \end{aligned} \tag{13}$$

where the relations $H(\sigma)H(\varepsilon) = 1$ for $c_x > c_0$ and $H(\sigma)H(-\varepsilon) = 1$ for $0 < c_x < c_0$ are substituted.

C. Sheath

The solution of (6) without source terms in the sheath yields $|c_x|g(x,\varepsilon,\sigma) = b(\varepsilon,\sigma)$. Hence, for a given total energy ε and direction, the ion distribution function is conserved. The boundary condition at the wall is

$$g(x_w,\varepsilon,-1) = g_w(\varepsilon,-1) + \rho g(x_w,\varepsilon,+1) \tag{14}$$

where ρ is the ion reflectivity. The other condition is the distribution function at the sheath edge g_b, which is obtained from the solution in the presheath. Because the ions experience turning in the sheath for total energy less than sheath edge potential, different ion distribution functions are presented as follows.

1) Total energy $\varepsilon \geq Z_i e\phi_b$. Owing to conservation of distribution functions, the ion distribution function in the forward direction is

$$\begin{aligned}|c_x|g(x,\varepsilon,+1) &= |c_{xw}|\,g(x_w,\varepsilon,+1) \\ &= |c_{xb}|\,g_b(\varepsilon,+1). \end{aligned} \tag{15}$$

The ion distribution function for the negative velocities by substituting (14) yields

$$\begin{aligned}|c_x|g(x,\varepsilon,-1) &= |c_{xw}|\,[g_w(\varepsilon,-1)+\rho g(x_w,\varepsilon,+1)] \\ &= |c_{xb}|\,g(x_b,\varepsilon,-1). \end{aligned} \tag{16}$$

2) Total energy $\varepsilon < Z_i e\phi_b$. Conservation of the ion distribution function in a given direction and at the turning point leads to

$$\begin{aligned} |c_x| g(x,\varepsilon,+1) &= |c_x| g(x,\varepsilon,-1) \\ &= |c_x| g(\varepsilon), \qquad \varepsilon < Z_i e\phi_b. \end{aligned} \tag{17}$$

Irrespective of directions and locations, ion distribution functions in the sheath, therefore, are the same for a given total energy. Introducing (14) into (17) gives

$$|c_x| g(x,\varepsilon,+1) = |c_{xw}| \left[g_w(\varepsilon,-1) + \rho g(x_w,\varepsilon,+1) \right]. \tag{18}$$

Evaluating at the wall, (18) becomes

$$g(x_w,\varepsilon,+1) = \frac{1}{1-\rho}\, g_w(\varepsilon,-1). \tag{19}$$

Combining (15), (16), (17), and (19), ion distribution functions in the forward and backward directions in the sheath are, respectively,

$$\begin{aligned} &|c_x| g(x,\varepsilon,+1) \\ &\quad = H(\varepsilon - Z_i e\phi_b)\, |c_{xb}|\, g_b(\varepsilon,+1) \\ &\qquad + H(Z_i e\phi_b - \varepsilon)\, \frac{1}{1-\rho}\, |c_{xw}|\, g_w(\varepsilon,-1) \end{aligned} \tag{20}$$

$$\begin{aligned} &|c_x| g(x,\varepsilon,-1) \\ &\quad = H(\varepsilon - Z_i e\phi_b) \left[|c_{xw}|\, g_w(\varepsilon,-1) \right. \\ &\qquad \left. + \rho\, |c_{xb}|\, g_b(\varepsilon,+1) \right] + H(Z_i e\phi_b - \varepsilon) \\ &\qquad \times \frac{1}{1-\rho}\, |c_{xw}|\, g_w(\varepsilon,-1). \end{aligned} \tag{21}$$

Ion distribution function $F_i = H(\sigma) m_i |c_x| g(\varepsilon,+1) + H(-\sigma) m_i |c_x| g(\varepsilon,-1)$ by substituting (20) and (21) leads to

$$\begin{aligned} \frac{F_i(x,c_x)}{m_i} &= H(c_x - c_0')\, |c_{xb}|\, g_b(\varepsilon,+1) + H(c_x) H(c_0' - c_x) \\ &\quad \times \frac{1}{1-\rho}\, |c_{xw}|\, g_w(\varepsilon,-1) + H(-c_x) H(c_0' + c_x) \\ &\quad \times \frac{1}{1-\rho}\, |c_{xw}|\, g_w(\varepsilon,-1) + H(-c_0' - c_x) \\ &\quad \times \left[|c_{xw}|\, g_w(\varepsilon,-1) + \rho\, |c_{xb}|\, g_b(\varepsilon,+1) \right], \end{aligned} \tag{22}$$

where the relations $H(\sigma)H(\varepsilon - Z_i e\phi_b) = 1$ for $c_x > c_0'$, $H(\sigma)H(Z_i e\phi_b - \varepsilon) = 1$ for $0 < c_x < c_0'$, $H(-\sigma)H(\varepsilon - Z_i e\phi_b) = 1$ for $c_x < -c_0'$, and $H(-\sigma)H(Z_i e\phi_b - \varepsilon) = 1$ for $-c_0' < c_x < 0$ are introduced.

D. Coupling Between Presheath and Sheath

Evaluating (21) at the sheath edge gives

$$\begin{aligned} &|c_{xb}|\, g_b(\varepsilon,-1) \\ &\quad = H(\varepsilon - Z_i e\phi_b) \left[\rho\, |c_{xb}|\, g_b(\varepsilon,+1) + |c_{xw}|\, g_w(\varepsilon,-1) \right] \end{aligned} \tag{23}$$

where the first term on the right-hand side is determined by evaluating (12) at the sheath edge. Equation (23), therefore, yields

$$\begin{aligned} &|c_{xb}|\, g_b(\varepsilon,-1) \\ &\quad = \frac{1}{1 - H(-c_{xb})\, H(c_{0b} + c_{xb})\, \rho e^{-(2\beta_b x_b - 2\beta_t x_t)}} \\ &\qquad \times \left\{ H(-c_{xb} - c_{0b})\, \rho \left[g_1(\varepsilon,+1)\, |c_{x_1}|\, e^{-(\beta_b x_b - \beta_1 x_1)} \right. \right. \\ &\qquad \left. + \int_{x_1}^{x_b} A(x',\varepsilon,+1) e^{-(\beta_b x_b - \beta' x')}\, dx' \right] \\ &\qquad + H(-c_{xb})\, H(c_{0b} + c_{xb})\, \rho \\ &\qquad \times \left[\int_{x_t(\varepsilon)}^{x_b} A(x',\varepsilon,-1) e^{-(\beta' x' + \beta_b x_b - 2\beta_t x_t)}\, dx' \right. \\ &\qquad \left. \left. + \int_{x_t(\varepsilon)}^{x_b} A(x',\varepsilon,+1) e^{-(\beta_b x_b - \beta' x')}\, dx' \right] \right. \\ &\qquad \left. + H(-c_{xb})\, |c_{xw}|\, g_w(\varepsilon,-1) \right\} \end{aligned} \tag{24}$$

where the relations $H(-\sigma)H(\varepsilon - Z_i e\phi_b)H(\varepsilon) = 1$ for $c_{xb} < -c_{0b}$, $H(-\sigma)H(\varepsilon - Z_i e\phi_b)H(-\varepsilon) = 1$ for $-c_{0b} < c_{xb} < 0$, and $H(-\sigma)H(\varepsilon - Z_i e\phi_b) = 1$ for $c_{xb} < 0$ are used.

E. Ion Density in Presheath

Ion density can be determined by

$$\begin{aligned} n_i(x) &= \int_0^\infty F_i(x,-c_x)\, dc_x + \int_0^\infty F_i(x,c_x)\, dc_x \\ &= \sum_\sigma \int_{\varepsilon_t(x)}^\infty g(x,\varepsilon,\sigma)\, d\varepsilon. \end{aligned} \tag{25}$$

It is useful to reverse the order of integration $dx'\, d\varepsilon$ to $d\varepsilon\, dx'$. Because the domain should be the same, domain surrounded by $x_t(\varepsilon)H(-\varepsilon) \le x' \le x_b$ and $\varepsilon_t(x) \le \varepsilon \le \infty$ can also be represented by $\varepsilon_{\min}(x') \le \varepsilon < \infty$ and $0 \le x' \le x_b$, where $\varepsilon_{\min}(x') \equiv \text{greater}[Z_i e\phi(x), Z_i e\phi(x')]$. Substituting $A(-x',\varepsilon,-1) = A(x',\varepsilon,-1) = A(x',\varepsilon,+1)$ [17], $\beta \equiv 0$ and $\rho = 0$, $g_w \equiv 0$ in an symmetric system (25) leads to the ion density equation provided by Scheuer and Emmert [17].

F. Electron (or Negative Ion) Distribution Function in the Sheath

The electrons experience turning in the sheath for a total energy less than the potential at the wall. The electron distribution function yields

$$\begin{aligned} F_e(x,c_x) &= H(c_x) m_e |c_x| g_e(x,\varepsilon,+1) \\ &\quad + H(-c_x) m_e |c_x| g_e(x,\varepsilon,-1) \end{aligned} \tag{26}$$

where distribution functions

$$\begin{aligned} &|c_x| g_e(x,\varepsilon,+1) \\ &\quad = H(\sigma)\, |c_{xb}|\, g_{eb}(\varepsilon,+1) \end{aligned} \tag{27}$$

$$
\begin{aligned}
&|c_x| g_e(x,\varepsilon,-1) \\
&\quad = H(-\sigma)\{H(\varepsilon+e\phi_w)[|c_{xw}|\, g_{ew}(\varepsilon,-1) \\
&\qquad + \rho_e |c_{xb}|\, g_{eb}(\varepsilon,+1)] \\
&\qquad + H(-e\phi_w-\varepsilon)|c_{xb}|\, g_{eb}(\varepsilon,+1)\}. \qquad (28)
\end{aligned}
$$

Substituting (27) and (28) into (26) leads to

$$
\begin{aligned}
F_e(x,c_x) &= H(c_x+c'_{e0}) m_e |c_{xb}|\, g_{eb}(\varepsilon,+1) \\
&\quad + H(-c_x-c'_{e0})[m_e |c_{xw}|\, g_{ew}(\varepsilon,-1) \\
&\quad + \rho_e m_e |c_{xb}|\, g_{eb}(\varepsilon,+1)] \qquad (29)
\end{aligned}
$$

which the relations $H(-\sigma)H(\varepsilon+e\phi_w)=1$ for $c_x<-c'_{e0}$ and $H(-\sigma)H(-\varepsilon-e\phi_w)=1$ for $-c'_{e0}<c_x<0$ are used. Equation (29) indicates that the electrons with velocities greater than critical velocity c'_{e0} result from the electrons across the sheath edge, whereas those greater than c'_{e0} in the negative direction are from the wall emission and reflection after contacting the wall.

G. Electrostatic Potential Versus Position—An Extension of Emmert et al.'s Model

The variation of electrostatic potential with position can be obtained by following the model and analysis from Emmert *et al.* [7]. This work further accounts for the wall partially reflecting ions and electrons. Aside from a quasisteady state and ignorance of electromagnetic force, as mentioned previously, the assumptions made are as follows.

1) The ion source function in the presheath is chosen to be that provided by Emmert *et al.* [7]. This model is based on the fact that the ions would be a Maxwell–Boltzmann distribution in the absence of an electrostatic field at the symmetric point in a plasma or far from the wall.
2) The presheath is collisionless. The results can also apply to the ion–ion collisions [17]. Collisionality in the presheath, unfortunately, is often marginal. That is, mean-free paths between the electrons and ions can be of the same magnitude as the thickness of the presheath. Modeling different kinds of atomic or molecular collisions is complicated and inaccurate.
3) Thermal, field, and secondary emissions of electrons from the wall are ignored. For copper or tungsten having a work function of 4.5 eV, emitted electrons evaluated from a T–F equation [18] are 10^6 A/m^2 for a typical temperature of 3000 K and electric field intensity 10^7 V/m. Current density is, therefore, one-tenth to one-hundredth of the total current predicted by Hsu and Pfender [19]. The secondary electron emission can be observed for bombardment by ions, electrons, and neutrals. Provided that the incident energies of ions, electrons, and neutrals are less than 1 eV or much greater than 10^5 eV, the surface of the wall is covered by a monolayer, or the microstructure exhibits crystalline directions, the secondary electron coefficient, or yield, indicating the number of electrons ejected per incident particle can be much less than unity [13]. Ion emission can be found by a similar equation [20].
4) Electron density in the presheath is of Maxwell–Boltzmann distribution. The error induced is within 1%, as discussed by Self [21] and Emmert *et al.* [7].

The ion source function in (3) proposed by Emmert *et al.* [7] is

$$
S_i(x',\varepsilon) = \frac{S_0 h(x')}{2k_B T_{i0}} \exp\left[-\frac{\varepsilon - Z_i e\phi(x')}{k_B T_{i0}}\right] \qquad (30)
$$

where the unknown function $h(x')$ includes spatial variations of temperature (in a local equilibrium sense), potential, and concentrations of ions, electrons, or neutrals. Temperature T_{i0} is the temperature at the location where potential $\phi = 0$ and fluid velocity $u = 0$. Substituting (30) and symmetric condition $g_1 = g_b$, ion distribution function in the presheath from (13) is simplified to

$$
\begin{aligned}
F_i(x,c_x) &= \frac{n_{e0}}{(1+\rho)Z_i}\sqrt{\frac{m_i}{2\pi k_B T_{i0}}}\exp\left(-\frac{\varepsilon}{k_B T_{i0}}\right) \\
&\quad \cdot \{H(c_x-c_0)\{K(\chi_b)+K(\chi) \\
&\qquad + \rho[K(\chi_b)-K(\chi)]\} \\
&\qquad + H(c_x)H(c_0-c_x)\{K(\chi_b)-2K(\chi_t) \\
&\qquad + K(\chi)+\rho[K(\chi_b)-K(\chi)]\} \\
&\qquad + H(-c_x)H(c_0+c_x)\{K(\chi_b)-K(\chi) \\
&\qquad + \rho[K(\chi_b)-2K(\chi_t)+K(\chi)]\} \\
&\qquad + H(-c_0-c_x)\{K(\chi_b)-K(\chi) \\
&\qquad + \rho[K(\chi_b)+K(\chi)]\}\}, \qquad (31)
\end{aligned}
$$

where function K is defined as [7]

$$
K(\chi) \equiv \frac{\pi B(Z_i\kappa+1)}{\sqrt{\pi Z_i\kappa}} \int_0^{\chi} h(\chi') e^{-Z_i\kappa\chi'} \frac{dx'}{d\chi'}\, d\chi'. \qquad (32)
$$

In (31), the critical velocity c_0 is defined as a particle released from $x=0$ has speed c_0 at location x. Evidently, four regions of the ion distribution function exist at location x. Equation (31) reduces to the ion distribution function of Emmert *et al.* [7] for a completely absorbing wall ($\rho = 0$). To find electrostatic potential in (32), electrical neutrality, $n_e = Z_i n_i$, in the presheath is needed. The ion and electron densities are, respectively

$$
n_i = \int_{-\infty}^{\infty} F_i\, dc_x, \qquad n_e = \int_{-\infty}^{\infty} F_e\, dc_x. \qquad (33)
$$

Substituting (13), (25) gives

$$
n_i(x) = \frac{2(1+\rho)}{1-\rho} \int_0^{x_b} \int_{\varepsilon_{\min}(x')}^{\infty} \frac{S_i(x',\varepsilon)}{|c_x|}\, d\varepsilon\, dx'. \qquad (34)
$$

Electron density is of a Maxwell–Boltzmann distribution

$$
n_e = n_{e0} \exp\left(\frac{e\phi}{k_B T_{e0}}\right). \qquad (35)
$$

Substituting (30) into (34), performing integration, and applying electrical neutrality by introducing (35) lead to a plasma equation

$$
e^{-\chi} = B\sqrt{\frac{\pi}{Z_i\kappa}}\,(Z_i\kappa+1)\int_0^{\chi_b} h(\chi') I(\chi-\chi') \frac{dx'}{d\chi'}\, d\chi' \qquad (36)
$$

where B is a constant and function I is defined as

$$I(\chi-\chi') \equiv e^{Z_i\kappa(\chi-\chi')}\{H(\chi-\chi')\,\mathrm{erfc}[\sqrt{Z_i\kappa(\chi-\chi')}] + H(\chi'-\chi)\}. \tag{37}$$

Equation (36) by substituting (37) and differentiating with respect to χ leads to

$$e^{-\chi} = B\int_0^{\chi} \frac{h(\chi')}{\sqrt{\chi-\chi'}}\,\frac{dx'}{d\chi'}\,d\chi' \tag{38}$$

which is the well-known Abel's integral equation [22]. The solution of (38), therefore, yields

$$\frac{dx'}{d\chi'} = \frac{1}{\pi B h(\chi')}\left[\frac{1}{\sqrt{\chi'}} - 2D\left(\sqrt{\chi'}\right)\right] \tag{39}$$

where the Dawson function [23] is defined as

$$D\left(\sqrt{\chi'}\right) = e^{-\chi'}\int_0^{\sqrt{\chi'}} e^{t^2}\,dt. \tag{40}$$

The Dawson integral defined by (40) is slightly different from that of Emmert *et al.* [7]. The Bohm criterion is automatically satisfied by differentiating (36) with respect to χ to obtain (38), as proved by Bissell [8]. A detailed derivation will be presented later. Substituting (39) into (32) and performing integration lead to

$$K(\chi)e^{Z_i\kappa\chi} = K(\chi_b)e^{Z_i\kappa\chi}\,\mathrm{erf}\left(\sqrt{Z_i\kappa\chi}\right) + \frac{2}{\sqrt{\pi Z_i\kappa}}D(\sqrt{\chi}). \tag{41}$$

Interestingly, K function is independent of unknown functions h and S_0. Emmert *et al.* [7] obtained the same results for a completely absorbing wall. Substituting (37) and (39) into (36) and integrating lead to

$$\frac{2}{\sqrt{\pi Z_i\kappa}}\,D(\sqrt{\chi_b}) = \mathrm{erfc}\left(\sqrt{Z_i\kappa\chi_b}\right)e^{Z_i\kappa\chi_b} \tag{42}$$

which is the same equation as obtained by Emmert *et al.* [7], even though ion reflection is taken into account. Equation (42) is also independent of potential and unknown function h appearing in (30). Equation (41) leads to $K(0)=0$ and $K(\chi_b)=1$. The latter is obtained by substituting (42) into (41) evaluated at the sheath edge.

H. The Bohm Criterion

Equation (31) at the sheath edge reduces to

$$\begin{aligned} F_{ib}(c_x) = {} & \frac{2n_{e0}}{(1+\rho)Z_i}\sqrt{\frac{m_i}{2\pi k_B T_{i0}}} \\ & \times \exp\left(-\frac{\varepsilon}{k_B T_{i0}}\right)\{H(c_x-c_0) \\ & + H(c_x)H(c_0-c_x)[1-K(\chi_t)] \\ & + H(-c_x)H(c_0+c_x)\rho[1-K(\chi_t)] \\ & + H(-c_0-c_x)\rho\}. \end{aligned} \tag{43}$$

Substituting (43) and conducting integration, the following identity is obtained:

$$\int_{-\infty}^{\infty}\frac{F_{ib}(c_x)}{c_x^2}\,dc_x = \frac{n_{e0}m_i}{Z_i^2 k_B T_{e0}}e^{-\chi_b} \tag{44}$$

which is the Bohm criterion satisfied marginally, irrespective of ion and electron reflectivities. Equation (44) can also be represented by

$$\frac{Z_i^2 e}{m_i}\int_{-\infty}^{\infty}\frac{F_{ib}(c_x)}{c_x^2}\,dc_x = \left(\frac{dn_e}{d\phi}\right)_{\phi=\phi_b} \tag{45}$$

which is the marginal form provided by Chen [1] and Bissell [8].

I. Distribution Functions in Sheath

The ion distribution function at location x can be readily obtained from (22) by ignoring wall emission

$$\frac{F_i(x,c_x)}{m_i} = H(c_x-c_0')\,|c_{xb}|\,g_b(\varepsilon,+1) + H(-c_0'-c_x)\rho\,|c_{xb}|\,g_b(\varepsilon,+1) \tag{46}$$

where the first term on the right-hand side represents the distribution function of the ions moving in the positive direction and the last term is the distribution function for the ions in the negative direction after hitting the wall. The distribution function of the forward-moving ions at the sheath edge from (31) yields

$$\begin{aligned} |c_{xb}|\,g_b(\varepsilon,+1) = {} & \frac{2n_{e0}}{m_i(1+\rho)Z_i}\sqrt{\frac{m_i}{2\pi k_B T_{i0}}}\exp\left(-\frac{\varepsilon}{k_B T_{i0}}\right) \\ & \times\{H(c_{xb}-c_0)\,K(\chi_b) + H(c_{xb}) \\ & \times H(c_0-c_{xb})\,[K(\chi_b)-K(\chi_t)]\} \end{aligned} \tag{47}$$

where the first term on the right-hand side is referred to high-energy ions ($\varepsilon > 0$) coming from the presheath edge and the ions ionized with positive velocities in the presheath, and the last term represents low-energy ions ($Z_i e\phi_b < \varepsilon < 0$) generated with positive velocities and negative velocities experiencing turning in the presheath.

Without wall emission, the electron distribution function in the sheath from (29) yields

$$F_e(x,c_x) = H(c_x+c_{e0}')m_e\,|c_{xb}|\,g_{eb}(\varepsilon,+1) + H(-c_x-c_{e0}')\rho_e m_e\,|c_{xb}|\,g_{eb}(\varepsilon,+1) \tag{48}$$

where the distribution function at the sheath edge

$$m_e\,|c_{xb}|\,g_{eb}(\varepsilon,+1) = n_{eb}\sqrt{\frac{m_e}{2\pi k_B T_{e0}}}\exp\left(-\frac{\varepsilon+e\phi_b}{k_B T_{e0}}\right). \tag{49}$$

The error and Dawson functions were numerically integrated by a Simpson's rule. Errors were less than 10^{-6} by comparing grids of 1000 and 500.

III. Results and Discussion

In this study, distribution functions of the ions and electrons in the presheath and sheath are determined from the Boltzmann equation. The electric field in the presheath is found by applying the condition of electrical neutrality and introducing the ion source model proposed by Emmert *et al.* [7]. The effects of ion reflectivity on dimensionless ion distribution functions in the presheath and sheath are shown in Fig. 2. Dimensionless potential, which is an increasing function of x-coordinate, is used to represent position, to avoid specifications of unknown function

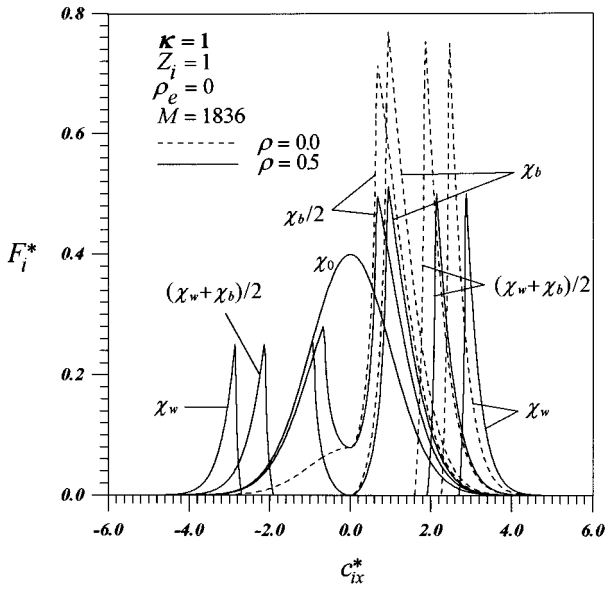

Fig. 2. Dimensionless distribution function (F_i^*) versus velocities (c_{ix}^*) of ions at different locations in presheath or sheath for different ion reflectivities of the wall (ρ).

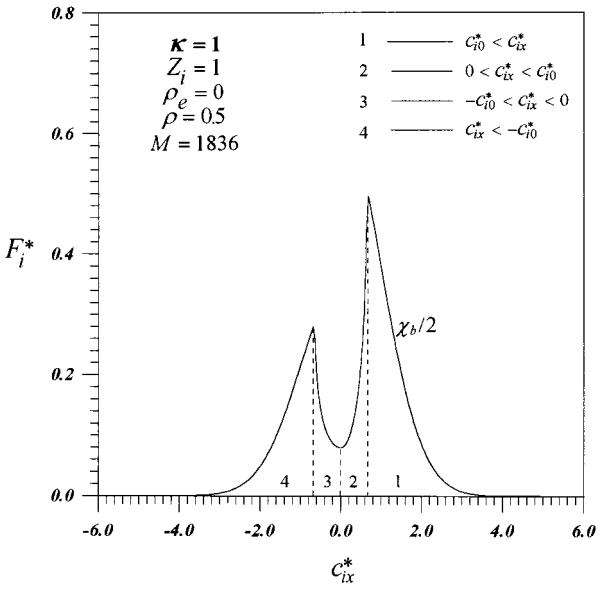

Fig. 3. Dimensionless distribution function (F_i^*) versus velocities (c_{ix}^*) of ions composed of the ions coming from different regions at location $\chi = \chi_b/2$ in presheath.

h [see (30)] and variations in temperature and ion source, and so on. Irrespective of ion reflectivity, the ions near the presheath edge or at the center of bulk plasma obey a Maxwell–Boltzmann distribution. This is because the effect of ion reflectivity on ion flow in the backward direction decays because of the retarding electric field. In the case of zero ion reflectivity, ion distribution functions in the presheath and sheath are found to be identical to those of Emmert *et al.* [7]. For a nonzero ion reflectivity, distribution functions in both the presheath and sheath exhibit two peaks, which are associated with positive and negative velocities, respectively. The ions near the peak with positive velocity are similar to those for zero ion reflectivity. The ions are composed of those coming from the presheath edge and the ions created with positive velocities in the backward region of the presheath, and the low-energy ions generated with negative velocities in the entire presheath. The ions close to the other peak come from the ions reflected by the wall and ions generated with negative velocities in the forward region. In the sheath, two peaks are separated by a gap, which is attributed to the ions having minimum energy equal to sheath edge potential. The gap widens because of an increase in ion speed in the forward direction. It is found that ion distribution functions at the sheath edge vanish at zero speed for different reflectivities. This is the requirement to avoid infinite potential [5]. If two-stream instability is accounted for, distortion of the distribution function can be ignored because of a local energy transport between the wave and particles having thermal velocities near the phase velocity or the wave having the phase velocity lying far in the tail of the distribution [1]. A systematic study of the relationships between different kinds of instabilities and distribution function is crucial.

The dimensionless distribution function at a typical location $\chi = \chi_b/2$ in the presheath can be divided into four parts, as shown in Fig. 3. The ions in part 1 have positive velocities $c_{ix}^* > c_{i0}^*$ (or $\varepsilon > 0$). They are the ions coming from the presheath edge and ions created with high positive velocities in the presheath. The ions in part 2 have low-energy with positive velocities $c_{ix}^* < c_{i0}^*$ (or $Z_i e\phi < \varepsilon < 0$). They are composed of ions created with positive velocities from the backward region and negative velocities experiencing turning in the presheath. Part 3 is for low-energy ions moving with negative velocities $c_{ix}^* > -c_{i0}^*$ (or $Z_i e\phi < \varepsilon < 0$). The ions include those created with positive velocities after reflection by the wall and those ionized with negative velocities in the forward region. Part 4 is for high-energy ions with negative velocities $c_{ix}^* < -c_{i0}^*$ (or $\varepsilon > 0$). They are composed of the ions reflected by the wall and created with high negative velocities in the forward region. The former includes the ions streaming into the presheath from the bulk plasma and ions generated with high positive velocities in the presheath.

The dimensionless ion distribution function at a given location in the sheath can be divided into six parts, as shown in Fig. 4. The ions in part 1 are composed of the ions coming from the bulk plasma and ions generated with high positive velocities in the presheath. Part 2 is for the ions created with total energy $Z_i e\phi_b < \varepsilon < 0$ in the presheath. No ions presented in parts 3 and 4, because no ions are generated in the sheath. In other words, ions across the sheath have the minimum energy equal to sheath edge potential. The ions in parts 5 and 6 are, respectively, those reflected by the wall from regions 2 and 1. Referring to Figs. 3 and 4, it is concluded that using Maxwell–Boltzmann distributions for ions to study transport process near a wall reflecting ions is inaccurate.

Spatial variations of electron distribution functions in the presheath and sheath for different electron reflectivities are presented in Fig. 5. It can be seen that electron distribution functions gradually become Maxwell–Boltzmann distribution in the backward direction toward the bulk plasma. Hence, for different electron reflectivities, electron distribution functions in the presheath $(0 < \chi < \chi_b)$ can be considered as

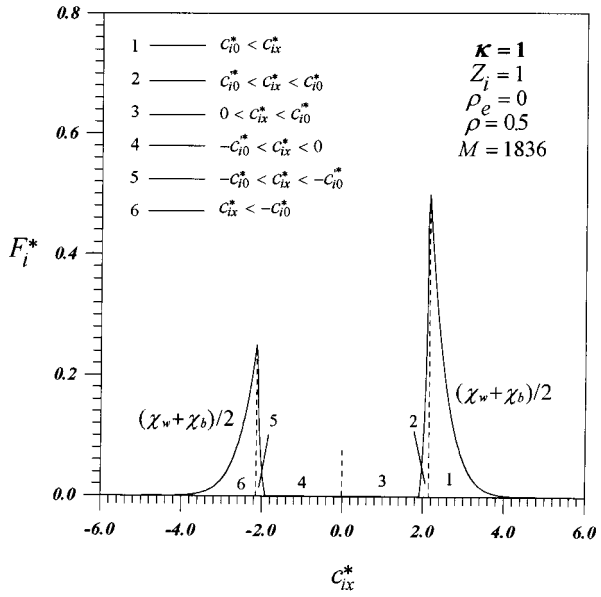

Fig. 4. Dimensionless distribution function (F_i^*) versus velocities (c_{ix}^*) of ions composed of the ions coming from different regions at location $\chi = (\chi_b + \chi_w)/2$ in sheath.

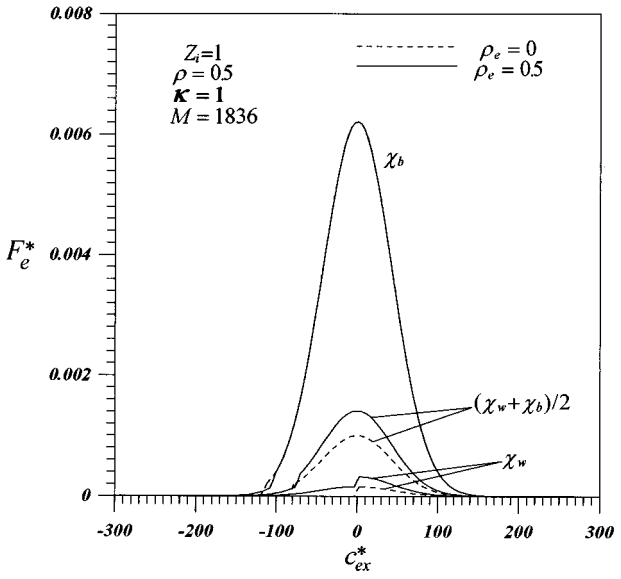

Fig. 5. Dimensionless distribution function (F_e^*) versus velocities (c_{ex}^*) of electrons at different locations in sheath for different electron reflectivities of the wall (ρ_e).

Maxwell–Boltzmann distributions. The distribution function at the sheath edge deviates slightly from a Maxwell–Boltzmann distribution in the tail region (for $c_{ex}^* < -100$). Because only the electrons that have high energy to overcome potential can hit the wall, the electrons in the tail region are those rebound by the wall and accelerated to high speeds. Errors induced for transport variables, which are obtained by integrating a distribution function, are therefore negligibly small. It is noted that for a wall emitting electrons, the distribution function also depends on surface conditions of the wall. Strong wall emission results in a significant deviation from a Maxwell–Boltzmann distribution. For a wall reflecting ions and electrons, the assumption of Maxwell–Boltzmann distributions for the electrons in the presheath is still relevant. On the other hand, electrons in the sheath $(\chi_b \leq \chi < \chi_w)$ deviate significantly from the Maxwell–Boltzmann distribution, because the tail region, as discussed previously, causes a large error (namely, the drop in the range of negative velocity) for a wall partially reflecting ions. Regardless of electron (and ion) reflectivity, the forward-moving electrons still obey a half part of the Maxwell–Boltzmann distribution.

The predicted transport variables, such as densities, fluid velocity, fluid-like conduction heat, difference between mean pressure and fluid-like viscous stress of the ions and electrons in the sheath from the moment equations of the ion and electron distribution functions provided by this work agree well with the available theoretical work from Schwager and Birdsall [24]. The results are shown in the companion paper [14].

IV. Conclusion

The conclusions drawn are as follows:

1) General solutions of the ion and electron distribution functions in a collisional presheath and collisionless sheath of a plasma in contact with a wall reflecting and emitting electrons and ions are presented. The collisions are simulated by the BGK model. To obtain the relationship between electrostatic potential with position, the successful ion source model from Emmert *et al.* is used. The ion and electron distribution functions in the presheath and sheath on a wall partially reflecting ions and electrons, therefore, can be exactly obtained.
2) Velocities of the ions near the wall partially reflecting ions are of highly non-Maxwell–Boltzmann distributions having two peaks associated with positive and negative velocities, respectively. The two peaks in the sheath are separated by a gap, which widens as the wall is approached.
3) Velocities of the electrons in the presheath can be of Maxwell–Boltzmann distribution, even though the wall reflects electrons and ions. In the sheath, the electron distribution drops sharply in a range of negative velocity because of the wall partially reflecting electrons.
4) The generalized Bohm criterion is derived and satisfied marginally (namely, with the equality sign), even though ion and electron reflectivities are accounted for.

References

[1] F. F. Chen, *Introduction to Plasma Physics*. New York: Plenum, 1974.
[2] D. Bohm, "Minimum ionic kinetic energy for a stable sheath," in *The Characteristics of Electrical Discharges in Magnetic Fields*, A. Guthrie and R. Wakerling, Eds. New York: McGraw-Hill, 1949, ch. 3, pp. 77–86.
[3] L. Tonks and I. Langmuir, "A general theory of the plasma of an arc," *Phys. Rev.*, vol. 34, pp. 876–922, 1929.
[4] K.-U. Riemann, "The influence of collisions on the plasma sheath transition," *Phys. Plasmas*, vol. 4, pp. 4158–4166, 1997.
[5] E. R. Harrison and W. B. Thompson, "The low pressure plane symmetric discharge," *Proc. Phys. Soc. Lond.*, vol. 74, pp. 145–152, 1959.
[6] P. N. Hu and S. Ziering, "Collisionless theory of a plasma sheath near an electrode," *Phys. Fluids*, vol. 9, pp. 2168–2179, 1966.
[7] G. A. Emmert, R. M. Wieland, A. T. Mense, and J. N. Davidson, "Electric sheath and presheath in a collisionless, finite ion temperature plasma," *Phys. Fluids*, vol. 23, pp. 803–812, 1980.

[8] R. C. Bissell, "The application of the generalized Bohm criterion to Emmert's solution of the warm ion collisionless plasma equation," *Phys. Fluids*, vol. 30, pp. 2264–2265, 1987.
[9] K.-U. Riemann, "The Bohm criterion and sheath formation," *J. Phys. D: Appl. Phys.*, vol. 24, pp. 493–518, 1991.
[10] G. Bachet, L. Chèrigier, and F. Doveil, "Ion velocity distribution function observations in a multipolar argon discharge," *Phys. Plasmas*, vol. 2, pp. 1782–1788, 1995.
[11] M. J. Goeckner, J. Goree, and T. E. Sheridan, "Laser-induced fluorescence characterization of a multidipole filament plasma," *Phys. Fluids B*, vol. 3, pp. 2913–2921, 1991.
[12] S. Takamura, M. Y. Ye, T. Kuwabara, and N. Ohno, "Heat flows through plasma sheaths," *Phys. Plasma*, vol. 5, pp. 2151–2158, 1998.
[13] B. Chapman, *Glow Discharge Processes, Sputtering and Plasma Etching*. New York: Wiley, 1980.
[14] P. S. Wei and F. B. Yeh, "Fluidlike transport variables in a kinetic, collisionless plasma near a surface with ion and electron reflections," *IEEE Trans. Plasma Sci.*, vol. 28, pp. 1232–1242, Aug. 2000.
[15] P. L. Bhatnagar, E. P. Gross, and M. Krook, "A model for collision processes in gases. I. Small amplitude processes in charged and neutral one-component systems," *Phys. Rev.*, vol. 94, pp. 511–525, 1954.
[16] G. H. Kim, N. Hershkowitz, D. A. Diebold, and M. H. Cho, "Magnetic and collisional effects on presheaths," *Phys. Plasmas*, vol. 2, pp. 3222–3233, 1995.
[17] J. T. Scheuer and G. A. Emmert, "A collisional model of the plasma presheath," *Phys. Fluids*, vol. 31, pp. 1748–1756, 1988.
[18] E. L. Murphy and R. H. Good, Jr., "Thermionic emission, field emission, and the transition region," *Phys. Rev.*, vol. 102, pp. 1464–1473, 1956.
[19] K. C. Hsu and E. Pfender, "Analysis of the cathode region of a free-burning high intensity argon arc," *J. Appl. Phys.*, vol. 54, pp. 3818–3324, 1983.
[20] L. P. Smith, "The emission of positive ions from tungsten and molybdenum," *Phys. Rev.*, vol. 35, pp. 381–395, 1930.
[21] S. A. Self, "Exact solution of the collisionless plasma-sheath equation," *Phys. Fluids*, vol. 6, pp. 1762–1768, 1963.
[22] N. N. Lebedev, I. P. Skalskaya, and Y. S. Uflyand, *Worked Problems in Applied Mathematics*. New York: Dover, 1965.
[23] M. Abramowitz and I. A. Stegun, Eds., *Handbook of Mathematical Functions with Formulas, Graphs, and Mathematical Tables*. Washington, D.C.: National Bureau of Standards, 1970.
[24] L. A. Schwager and C. K. Birdsall, "Collector and source sheaths of a finite ion temperature plasma," *Phys. Fluids B*, vol. 2B, pp. 1057–1068, 1990.

Peng-Sheng Wei (M'00) received the M.S. degree in power mechanical engineering department from National Tsing Hua University, Hsinchu, Taiwan, R.O.C., in 1978, and the Ph.D. in mechanical engineering department from University of California at Davis in 1984.

He has been a Professor of mechanical engineering department in National Sun Yat-Sen University, Kaohsiung, Taiwan, R.O.C., since 1989. His research interests are heat transfer, fluid mechanics, phase change, and metals processing including processes and defects of welding, casting and surface heat treatment.

Feng-Bin Yeh received the B.S. degree in aerospace engineering department from Tamkang Univeristy, Taipei, Taiwan, R.O.C., in 1988, and the M.S. degree in mechanical engineering from NSYSU in 1990.

He is currently a Ph.D. student in mechanical engineering, NSYSU, and is also an engineer in the quality control division of Tang Eng Stainless Steel Plant, Kaohsiung. His research interests are heat transfer, fluid mechanics, and rapid solidification in metals processing.

Ching-Yen Ho received the B.S. degree in mechanical engineering department from National Chung-Hsing University, Taichung, Taiwan, ROC, in 1985, and the M.S. and Ph.D. degrees in mechanical engineering department from NSYSU in 1988 and 1997, respectively.

He was a faculty of mechanical engineering department in Wu Feng College of Technology and Commerce during 1988–1997. He has been an associate Professor of mechanical engineering department in Hwa Hsia College of Technology and Commerce, Taipei, since 1997. His current research interests are laser and electron beam machining, conduction, convection and radiative heat transfer, and solidification.